

Lie algebraic quantum phase reduction based on heterodyne detection

Wataru Setoyama* and Yoshihiko Hasegawa†
*Graduate School of Information Science and Technology,
The University of Tokyo, Tokyo 113-8656, Japan*
(Dated: June 28, 2024)

Measurement backaction inherently alters observed dynamics in quantum physics. In the realm of quantum synchronization, this backaction induces a phase bias, making the assessment of synchronization critically dependent on the choice of the observables. In this study, we extend the quantum phase reduction approach [PhysRevLett.132.093602] into heterodyne detection, offering a comprehensive theoretical framework for analyzing quantum synchronization dynamics through uniform continuous measurement over all possible quadrature observables. This method averages out the backaction, allowing for unbiased evaluation of synchronization between quantum oscillators while avoiding measurement-induced phase bias. Furthermore, by defining the phase and limit-cycle solution independently of specific observables, our proposed method consistently adapts to the scenario where the observables are freely modified during the time evolution. Through simulations of noise-induced synchronization, our method reveals that the number of phase clusters between oscillators is restricted by their bosonic levels.

I. INTRODUCTION

Synchronization, the alignment of an internal rhythm with external perturbations, is ubiquitous in nature, seen in firing neurons, oscillating laser beams, and Josephson junctions [1–4]. With the recent advancements in quantum technology, nanoscale oscillators have become a subject of study, encompassing superconducting circuits [5, 6], optomechanical oscillators [7, 8], atomic systems [9, 10], and quantum thermal machines [11–14]. The study of synchronization in nanoscale systems offers significant promise for advancing quantum technologies such as quantum metrology, communication, cryptography, and clock [15–18]. For instance, investigations into quantum clocks have demonstrated that the continuously monitored coupled quantum oscillators can yield more precise temporal information than classical clocks [18]. Thus, investigating synchronization within the quantum regime presents substantial technological possibilities. Regarding this issue, the quantum models of limit-cycle oscillators (i.e., nonlinear systems exhibiting self-sustained oscillation) are proposed, including qubit and spin oscillators [19, 20] and quantum van der Pol oscillators [21, 22]. Additionally, experimental research has shown evidence of quantum synchronization in limit-cycle oscillators in laboratory conditions [23–25].

Phase reduction is a standard theoretical scheme for studying synchronization dynamics, reducing weakly perturbed multi-dimensional limit-cycle dynamics to one-dimensional phase dynamics [1, 2]. Using Lie algebra, we introduced phase reduction method to quantum systems, providing a comprehensive framework for analyzing synchronization of quantum limit-cycle oscillators [26]. In a continuous measurement scheme of their coupled environment, quantum trajectories of these oscillators come

to follow a stochastic Schrödinger equation [27–29]. Provided that the disturbance of quantum noise is weak, these trajectories fluctuate around a limit-cycle solution. Based on the Lie algebraic framework, we calculated the phase response curves to weak perturbations represented by unitary transformations. Thus, a quantum phase equation was derived from a stochastic Schrödinger equation of a quantum limit-cycle oscillator. This approach is versatile from classical to quantum regimes and applicable to general quantum limit-cycle oscillators, including qubits and spins, lacking classical limit-cycle analogues. Note that the extension of phase reduction to quantum systems was pioneered in Ref. [30], relying on a semiclassical approximation, in which the quantum oscillators are approximated by their classical counterparts in the weak quantum regime.

Nonetheless, measurement backaction itself alters dynamics of quantum trajectories, resulting in the emergence of a phase bias. Hence, assessment of synchronization through a phase distribution hinges upon the choice of quadrature observables to be continuously measured. In fact, we reported that continuous homodyne measurement of quadratures induces phase biases, even in the absence of synchronization in Ref. [26]. It is unclear which quadratures should be chosen and measured to representatively evaluate synchronization. Furthermore, the quantum phase reduction approach defined the phase and limit-cycle solution according to a stochastic Schrödinger equation associated with fixed quadratures, leading to incompatibility between cases where different quadratures are continuously monitored.

In this study, we extend the quantum phase reduction approach to heterodyne detection, which involves continuous measurement uniform over all possible quadratures. Averaging out the measurement backaction for all quadrature angles, an unbiased quantum phase equation is derived from the stochastic Schrödinger equation based on heterodyne detection. Thus, the proposed method evaluates synchronization avoiding the

* setoyama@biom.t.u-tokyo.ac.jp

† hasegawa@biom.t.u-tokyo.ac.jp

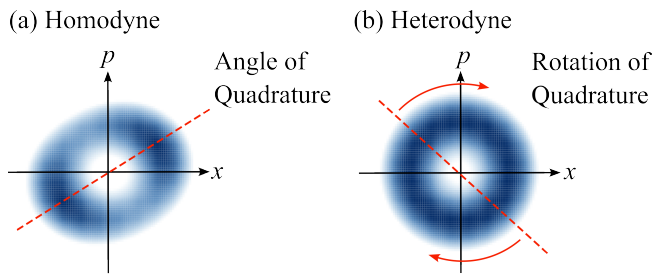


FIG. 1. Distributions of quantum states in homodyne and heterodyne detection. (a) Homodyne detection, where quadratures to be continuously monitored are fixed at certain angles, resulting in the biased distribution of quantum states due to their measurement backaction. (b) Heterodyne detection with quadratures rotating at sufficiently high frequency, allowing the unbiased distribution by averaging out measurement backaction across all angles of quadratures.

measurement-induced phase bias. For quantum van der Pol oscillators [21], we establish that the limit-cycle solution exhibits harmonic oscillation and that the measurement backaction induces no phase bias in heterodyne detection. Moreover, our proposed method defines the limit-cycle solution, phase, and phase response curve independently of any specific quadratures due to the uniform continuous measurement. By introducing these definitions from heterodyne to homodyne detection, the phase equation equally evaluates the measurement backaction for arbitrary quadratures. Therefore, the proposed approach handles scenarios where the measured quadratures vary during the time evolution and where quantum oscillators are continuously monitored by different quadratures. Additionally, we demonstrate the efficacy of our method through numerical simulations, where uncoupled quantum oscillators subjected to common noise exhibit synchronization or yield phase clusters. As a phenomenon not observed in classical synchronization, we reveal that the bosonic levels of these oscillators bound the possible number of the phase clusters between them; this limit is computed using the phase response curves.

II. METHODS

A. Stochastic Schrödinger equation for heterodyne detection

In open quantum systems, quantum limit-cycle oscillators are generally described by the Lindblad equation as follows [31, 32]:

$$\frac{d\rho}{dt} = -i[H, \rho] + \sum_{k=1}^K \mathcal{D}[L_k]\rho, \quad (1)$$

where H is Hamiltonian operator, L_k are the jump operators and $\mathcal{D}[L]\rho$ is dissipator defined by $\mathcal{D}[L]\rho \equiv L\rho L^\dagger -$

$(1/2)(L^\dagger L\rho + \rho L^\dagger L)$. However, the Lindblad equation describes the evolution of density operators of quantum systems, not that of the physically observable quantum states, known as quantum trajectory [33]. Quantum trajectories are the pure-state trajectories described by a stochastic Schrödinger equation with the associated currents in the continuous measurement of the environment to which the quantum systems are coupled. For continuous measurement, we use heterodyne detection for the quantum phase reduction in this paper, unlike our prior study based on homodyne detection. Figure 1 illustrates the difference between homodyne and heterodyne detection. In homodyne detection, we select the angles for continuously measuring the quadratures corresponding to jump operators L_k , resulting in the measurement backaction biased according to these angles, as depicted in Fig. 1(a). Conversely, for heterodyne detection, the measured quadratures are rotated at constant frequencies. As the rotation reaches a sufficient frequency, the measurement backaction is uniformly distributed over all quadrature angles, as shown in Fig. 1(b). Before introducing the quantum trajectory theory for heterodyne detection, we revisit that of homodyne detection, as the heterodyne stochastic Schrödinger equation is generally derived from the homodyne counterpart [34]. Two main approaches to implementation of homodyne detection exist: detection of stochastic homodyne currents by physical detectors [28] and continuous application of weak Gaussian measurements [35]. Quantum trajectories have been experimentally observed in various devices, such as cavities [36], superconducting circuits [37], and mechanical resonators [38]. In homodyne detection, the quantum trajectories obey the following stochastic Schrödinger equation in the Stratonovich form [27–29]:

$$\begin{aligned} d|\psi\rangle = & \left[-iH + \sum_{k=1}^K -\frac{1}{2}(X_k L_k - \langle X_k L_k \rangle) \right. \\ & \left. + \langle X_k \rangle (L_k - \langle L_k \rangle) \right] |\psi\rangle dt \\ & + \sum_{k=1}^K (L_k - \langle L_k \rangle) |\psi\rangle \circ dW_k, \end{aligned} \quad (2)$$

where \circ represents the Stratonovich calculus and $X_k \equiv L_k + L_k^\dagger$ is the quadrature corresponding to the jump operator L_k . Furthermore, $\langle O \rangle$ represents the expectation value of O in the state $|\psi\rangle$, that is, $\langle O \rangle \equiv \langle \psi | O | \psi \rangle$. The random variables dW_k are Wiener increments that satisfy $\mathbb{E}[dW_k] = 0$ and $\mathbb{E}[dW_m dW_n] = \delta_{mn} dt$, where $\mathbb{E}[\cdot]$ represents the average over all possible quantum trajectories. The homodyne current $J_{\text{hom},k}$ associated with the quadrature X_k is defined as $J_{\text{hom},k} \equiv \langle X_k \rangle + \xi_k(t)$, where $\xi_k(t) \equiv dW_k/dt$. The average of all possible quantum trajectories described by Eq. (2), that is, $\rho = \mathbb{E}[|\psi\rangle \langle \psi|]$, satisfies the Lindblad equation [Eq. (1)]. It is noteworthy that a stochastic Schrödinger equation satisfying the Lindblad equation is not unique, as the quadratures X_k can be measured at any angles. The rotation

TABLE I. Correspondence between classical and Lie-algebraic quantum phase reduction methods.

	Classical	Quantum
Space	Euclidean space	Hilbert space
Differential equation	(Stochastic) differential equation	Stochastic Schrödinger equation
Phase response curve	Gradient	Lie algebra
Perturbation	Vector	Unitary transformation

of the selected quadratures equals $U(1)$ transformation: $L_k \rightarrow L_k \exp(i\lambda_k)$, under which Eq. (1) remains invariant, and all forms of the stochastic Schrödinger equations also satisfy Eq. (1) as well, where λ_k is an arbitrary real parameter. This transformation is physically implemented by rotation of the local oscillator signal [28].

To average out the measurement backaction, we consider heterodyne detection in the fast rotation limit. By rotating the local oscillators with constant frequencies Ω_k , the jump operators L_k also oscillate with such frequencies as: $L_k \rightarrow \exp(i\Omega_k t)L_k$. As the frequency Ω_k increases to infinity, the backaction is averaged over the $U(1)$ transformation of L_k . In the fast rotation limit, the stochastic Schrödinger equation in heterodyne detection is derived from Eq. (2) as follows [34]:

$$\begin{aligned}
d|\psi\rangle &= \left(-iH_{\text{eff}} + \sum_{k=1}^K \frac{1}{2} \langle L_k^\dagger L_k \rangle + \langle L_k^\dagger \rangle (L_k - \langle L_k \rangle) \right) |\psi\rangle dt \\
&\quad + \sum_k (L_k - \langle L_k \rangle) |\psi\rangle \circ d\tilde{W}_k^*, \tag{3}
\end{aligned}$$

where $H_{\text{eff}} \equiv H - (i/2) \sum_k L_k^\dagger L_k$ is a non-Hermitian operator, called the effective Hamiltonian, and $d\tilde{W}_k \equiv (1/\sqrt{2})(dW_{k1} + idW_{k2})$ is the complex Wiener increment satisfying $E[d\tilde{W}_k] = 0$, $E[d\tilde{W}_m d\tilde{W}_n] = 0$, and $E[d\tilde{W}_m^* d\tilde{W}_n] = \delta_{m,n} dt$. The measured heterodyne current is $J_{\text{het},k} \equiv \langle L_k \rangle + \tilde{\xi}_k(t)$, where $\tilde{\xi}_k(t) \equiv d\tilde{W}_k/dt$. It is easily shown that the heterodyne stochastic Schrödinger equation [Eq. (3)] is independent of any specific quadratures, from the fact that Eq. (3) is invariant under arbitrary $U(1)$ transformation.

B. Phase reduction based on heterodyne detection

Prior to discussing the specifics of its extension to heterodyne detection, let us briefly revisit the concept of Lie algebraic quantum phase reduction [26]. This method is a general framework for quantum synchronization, reducing multi-dimensional dynamics of quantum trajectories of the quantum limit-cycle oscillators, which fluctuate in the vicinity of a deterministic limit-cycle solution in the Hilbert space, into one-dimensional phase dynamics. We separate the limit-cycle solution from the stochastic Schrödinger equation and define the phase both on and outside this limit-cycle solution. Additionally, the phase response curves, which represent the variation of

the phase in response to sufficiently weak unitary transformations, are computed using Lie algebra framework. Based on these definitions, the one-dimensional phase equation composed of the natural frequency of the limit-cycle solution and the phase response curves is derived from the stochastic Schrödinger equation. Table I shows the correspondence between the conventional and quantum phase reduction methods. Despite the difference between homodyne and heterodyne detection, the derivation process of the phase equation in this study follows that of the prior study [26].

To begin with, we define the limit-cycle solution for the stochastic Schrödinger equation [Eq. (3)]. As an analog of classical cases [39–42], we propose to remove noise terms from a stochastic Schrödinger equation in the Stratonovich form. The resulting equation is defined as deterministic dynamics, which converges to a limit-cycle solution:

$$\begin{aligned}
d|\psi\rangle &= \left(-iH_{\text{eff}} + \sum_{k=1}^K \frac{1}{2} \langle L_k^\dagger L_k \rangle + \langle L_k^\dagger \rangle (L_k - \langle L_k \rangle) \right) |\psi\rangle dt. \tag{4}
\end{aligned}$$

Although numerous stochastic calculi exist, we define the limit-cycle solution solely based on the Stratonovich calculus, as it uniquely satisfies the norm preservation of the limit-cycle solution and the chain rule of differentiation [26]. To be defined as a physical trajectory like quantum trajectories, the limit-cycle solution should be a pure-state trajectory or satisfy norm preservation. Equation (4), derived based on the Stratonovich calculus, satisfies $d\|\psi\| = 0$, where $\|\psi\| \equiv \sqrt{\langle \psi | \psi \rangle}$, while the deterministic term of the stochastic Schrödinger equation specified by any other stochastic calculus does not (see Appendix A for details). Additionally, the phase reduction approach generally requires a coordinate transformation between a state vector (corresponding to the quantum state $|\psi\rangle$ in this study) and a phase coordinate [43]. This transformation follows the chain rule of differentiation, which is uniquely satisfied in the Stratonovich calculus. The state $|\psi\rangle$ converges to the limit-cycle solution $|\psi_0\rangle$ when Eq. (4) satisfies the following condition,

$$\lim_{t \rightarrow \infty} |\langle \psi(t) | \psi(t+T) \rangle| = 1, \tag{5}$$

where T denotes the period of the limit-cycle solution. Note that the state $|\psi\rangle$ is physically equivalent under the $U(1)$ transformation: $|\psi\rangle \rightarrow \exp(i\lambda) |\psi\rangle$.

Next, we define the phase for the quantum states in the Hilbert space using the limit-cycle solution $|\psi_0\rangle$. On the limit-cycle solution, we define the phase θ to change at constant frequency $\omega = 2\pi/T$ under Eq. (4). Furthermore, by employing the isochrone, the phase θ can be defined outside of the limit-cycle solution as follows:

$$\Theta[|\psi(t)\rangle] = \lim_{n \rightarrow \infty} \Theta[|\psi(t + nT)\rangle], \quad (6)$$

where $\Theta[|\psi\rangle]$ represents the phase of the state $|\psi\rangle$ and the state $|\psi\rangle$ evolves according to Eq. (4). Because the limit-cycle dynamics [Eq. (4)] is invariant under the $U(1)$ transformation: $L_k \rightarrow \exp(i\lambda_k)L_k$, we can define the limit-cycle solution and phase regardless of any specific quadratures, unlike in our prior study based on homodyne detection.

It should be noted that the phase response curves for quantum limit-cycle oscillators are calculated with respect to Lie algebra generators, rather than the basis vectors in the Euclidean space as in the conventional phase reduction approach [1]. Arbitrary infinitesimal change of a pure state can be described by infinitesimal unitary transformation U , which can be decomposed into Lie algebra generators by the Taylor expansion as follows:

$$U = \exp\left(\sum_{l=1}^{N^2-1} -ig_l E_l - ig_0 I\right) \simeq I - \sum_{l=1}^{N^2-1} ig_l E_l - ig_0 I, \quad (7)$$

where I is an identity matrix, E_l are Lie algebra generators of $SU(N)$, and real coefficients g_l satisfies $|g_l| \ll 1$. The generators E_l of $SU(N)$ are bases of traceless $N \times N$ Hermitian operators, for example, corresponding to Pauli matrices when $N = 2$ and to Gell-Mann matrices when $N = 3$ (see Appendix B for details). Therefore, the phase response curve with respect to the generator E_l is defined as follows:

$$Z_l(\theta) \equiv \lim_{g_l \rightarrow 0} \frac{\Theta[\exp(-ig_l E_l) |\psi_0(\theta)\rangle] - \Theta[|\psi_0(\theta)\rangle]}{g_l}, \quad (8)$$

where $|\psi_0(\theta)\rangle$ represents the state $|\psi\rangle$ on the limit-cycle solution $|\psi_0\rangle$ with the phase θ . Equation (8) represents a partial differentiation of the phase θ with respect to a unitary transformation by the generator E_l . In the following, we assume that the perturbation is sufficiently weak such that the state $|\psi\rangle$ remains near the limit-cycle solution $|\psi_0\rangle$ and can be approximated by $|\psi_0(\Theta[|\psi\rangle])\rangle$.

Although the heterodyne stochastic Schrödinger equation [Eq. (3)] is not explicitly presented as a linear equation of Hermitian operators, this equation can be decomposed into Lie algebra generators due to its nonlinearity, as we show below. Generally, a pure-state dynamics is described by a linear operator as follows:

$$d|\psi\rangle = -iB|\psi\rangle dt, \quad (9)$$

where B is an arbitrary linear operator. Under Eq. (9), derivative of the norm $\langle\psi|\psi\rangle$ is represented as follows:

$$\begin{aligned} d(\langle\psi|\psi\rangle) &= (\langle\psi| + d\langle\psi|)(|\psi\rangle + d|\psi\rangle) - \langle\psi|\psi\rangle \\ &= d(\langle\psi|)|\psi\rangle + \langle\psi|d(|\psi\rangle) + d(\langle\psi|)d(|\psi\rangle) \\ &= -i\langle(B - B^\dagger)\rangle dt, \end{aligned} \quad (10)$$

where terms less than $O(dt)$ are neglected. When B is independent of the state $|\psi\rangle$, the norm preservation for arbitrary state $|\psi\rangle$ is satisfied only if B is an Hermitian operator as $B = B^\dagger$. On the other hand, when B is dependent on the state $|\psi\rangle$, that is, when Eq. (9) is nonlinear, the norm preservation for arbitrary state $|\psi\rangle$ can be satisfied even if B is not an Hermitian operator. Indeed, the norm-preserved dynamics described by non-Hermitian operators, such as Eqs. (3) and (4), can also be represented by an Hermitian operator as follows:

$$-i[B(|\psi\rangle) - \langle B(|\psi\rangle)\rangle]|\psi\rangle dt = -iH_B(|\psi\rangle)|\psi\rangle dt, \quad (11)$$

where H_B is the Hermitian operator

$$H_B(|\psi\rangle) \equiv [B(|\psi\rangle) - \langle B(|\psi\rangle)\rangle]|\psi\rangle\langle\psi| + \text{H.c.} \quad (12)$$

This statement holds true for the Stratonovich calculus. It should be noted that the term $-i\langle B\rangle|\psi\rangle dt$, the difference between Eqs. (9) and (11), can be neglected since it corresponds to $U(1)$ transformation, which has no physical effect on the state $|\psi\rangle$. Therefore, the heterodyne stochastic Schrödinger equation [Eq. (3)] and Eq. (4) can also be expressed as unitary transformations by the Hermitian operators $H_B(|\psi\rangle)$.

To derive the phase equation from the heterodyne stochastic Schrödinger equation [Eq. (3)], we focus on the stochastic terms of Eq. (3), since the deterministic term of Eq. (3) corresponds merely to the natural frequency ω in the phase dynamics. By following the procedure outlined in Eqs. (9)-(12), the stochastic terms of Eq. (3) can be represented by Hermitian operators as follows:

$$\begin{aligned} (L_k - \langle L_k\rangle)|\psi\rangle \circ d\tilde{W}_k^* \\ = -iH_{k1}(|\psi\rangle)|\psi\rangle \circ dW_{k1} - iH_{k2}(|\psi\rangle)|\psi\rangle \circ dW_{k2}, \end{aligned} \quad (13)$$

where $H_{k1}(|\psi\rangle)$ and $H_{k2}(|\psi\rangle)$ are the traceless Hermitian operators

$$H_{k1}(|\psi\rangle) \equiv \frac{i}{\sqrt{2}}(L_k - \langle L_k\rangle)|\psi\rangle\langle\psi| + \text{H.c.}, \quad (14)$$

$$H_{k2}(|\psi\rangle) \equiv \frac{1}{\sqrt{2}}(L_k - \langle L_k\rangle)|\psi\rangle\langle\psi| + \text{H.c.} \quad (15)$$

The stochastic terms of Eq. (3) are converted into the two orthogonal terms corresponding to the measurement backaction. The traceless Hermitian operator H_{km} can be decomposed into Lie algebra generators as $H_{km} = \sum_{l=1}^{N^2-1} g_{km,l} E_l$, where the coefficients $g_{km,l}$ are defined as $g_{km,l} \equiv \text{Tr}[H_{km} E_l]$ due to trace orthogonality of Lie

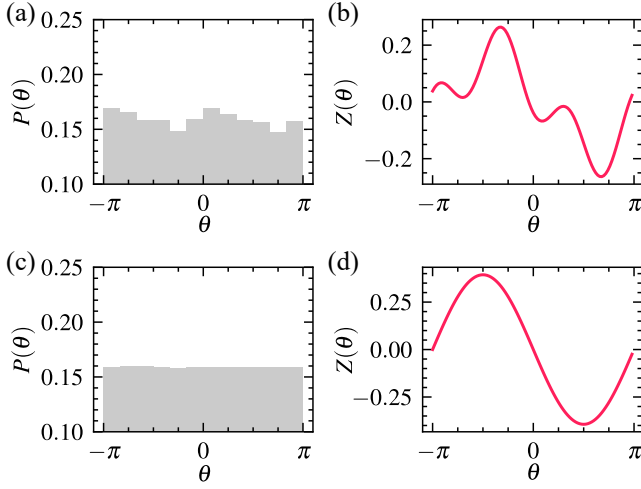


FIG. 2. Phase distribution $P(\theta)$ in steady state and phase response curve $Z(\theta)$ of quantum van der Pol oscillators in homodyne and heterodyne detection. (a) and (c) Phase distribution in (a) heterodyne detection and (c) homodyne detection. (b) and (d) phase response curve with respect to a harmonic drive in (b) heterodyne detection and (d) homodyne detection. The gray histograms are computed from simulations of the stochastic Schrödinger equation. The parameters are $(\Delta, \gamma_g, \gamma_d) = (1.0, 0.2, 1.0)$. The phase response curve with respect to the harmonic drive is calculated for an Hermitian operator $i(a - a^\dagger)$.

algebra generators. Then, the following phase equation is derived according to the chain rule of differentiation.

$$\frac{d\theta}{dt} = \omega + \sum_{k=1}^K \sum_{m=1}^2 \sum_{l=1}^{N^2-1} Z_l(\theta) g_{km,l}(\theta) \circ \xi_{km}(t), \quad (16)$$

where $g_{km,l}(\theta)$ is evaluated at $|\psi\rangle = |\psi_0(\theta)\rangle$ on the limit-cycle solution. The phase equation (16) in the Stratonovich form can be converted into an equivalent equation in the Ito form (see Appendix C for details).

$$\begin{aligned} \frac{d\theta}{dt} = & \omega + \frac{1}{2} \sum_{k=1}^K \sum_{m=1}^2 \frac{dY_{km}(\theta)}{d\theta} Y_{km}(\theta) \\ & + \sum_{k=1}^K \sum_{m=1}^2 Y_{km}(\theta) \xi_{km}(t), \end{aligned} \quad (17)$$

where $Y_{km}(\theta) \equiv \sum_{l=1}^{N^2-1} Z_l(\theta) g_{km,l}(\theta)$.

To demonstrate that the phase equation [Eq. (16)] is unbiased and independent of specific quadratures, we consider the case of a quantum van der Pol oscillator in heterodyne detection as an example. The Lindblad equation of the quantum van der Pol oscillator is represented as follows [21]:

$$\frac{d\rho}{dt} = -i[\Delta a^\dagger a, \rho] + \gamma_g \mathcal{D}[a^\dagger]\rho + \gamma_d \mathcal{D}[a^2]\rho, \quad (18)$$

where Δ is the detuning between the oscillator and the frequency of a rotating frame, a and a^\dagger are annihilation

and creation operators, respectively, and γ_g and γ_d are the jump rates corresponding to one-particle gain and two-particle loss, respectively. Owing to its $U(1)$ symmetry, we establish that, if it exists, the limit-cycle solution of the quantum van der Pol oscillators obtained according to Eq. (4) is always harmonic oscillation; the limit-cycle solution is not distorted at any specific angles of the measured quadratures (see Appendix D for details). Based on this limit-cycle solution, we calculate the phase response curves for each jump operator, by following Eqs. (13)-(15); for both jump operators, they correspond to first- and second-harmonic orthogonal trigonometric functions, respectively. According to Eq. (16), we derive the phase equation corresponding to the quantum van der Pol model as follows:

$$\begin{aligned} \frac{d\theta}{dt} = & \omega + v_1 \sin \theta \circ \xi_{11} + v_1 \cos \theta \circ \xi_{12} \\ & + v_2 \sin 2\theta \circ \xi_{21} + v_2 \cos 2\theta \circ \xi_{22} \\ = & \omega + v\xi, \end{aligned} \quad (19)$$

where v_1 and v_2 are the backaction strengths corresponding to one-particle gain and two-particle loss, respectively, and $v \equiv \sqrt{v_1^2 + v_2^2}$. The transition from the first to the second line utilizes the relation $\sum_{k=1}^K v_k dW_k = \sqrt{\sum_{k=1}^K v_k^2} dW$. Consequently, in the phase equation, the averaged backaction in heterodyne detection is simple white noise and serves as constant phase diffusion, while it induces clustering in homodyne detection (see Appendix E for details). Figure 2 illustrates the phase distribution in the steady state and the phase response curve with respect to the harmonic drive both in homodyne and heterodyne detection. In homodyne detection, clustering occurs in the steady state even without external drive in Fig. 2(a); however, no clustering is observed in heterodyne detection, as depicted in Fig. 2(c). Furthermore, while the previous method based on homodyne detection demonstrates a distorted phase response curve in Fig. 2(b), the proposed method for heterodyne detection shows an undistorted sinusoidal wave in Fig. 2(d). This can be attributed to the fact that, in the proposed method, the phase is independent of the quadratures and symmetric against rotation.

C. Application of phase reduction based on heterodyne detection to homodyne detection

As the definition of the phase depends on the fixed quadratures, Lie algebraic phase reduction based on homodyne detection [26] does not apply to the scenario where the measured quadratures are modulated. To address this issue, we apply the definition of the phase in the proposed method for heterodyne detection, which is independent of any quadratures, to homodyne detection. This application does not imply the introduction of an additional phase reduction approach specifically for ho-

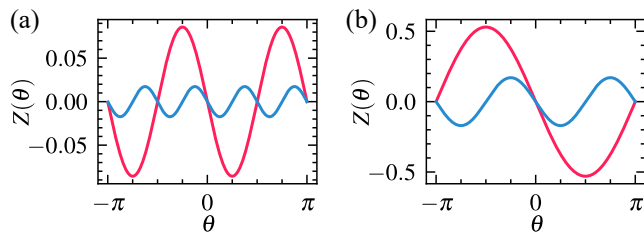


FIG. 3. Phase response curves of quantum van der Pol oscillator in homodyne detection. Phase response curves with respect to the measurement backaction corresponding to $L_1 = \sqrt{\gamma_1}a^\dagger$ (red line) and $L_2 = \sqrt{\gamma_2}a^2$ (blue line) for (a) deterministic and (b) stochastic terms. The parameters are $(\Delta, \gamma_g, \gamma_d) = (1.0, 0.2, 1.0)$.

modyne detection, distinct from the one proposed in Subsec. II B for heterodyne detection.

To derive the phase equation from the homodyne stochastic Schrödinger equation [Eq. (2)] based on the proposed method, we focus on the difference between Eq. (2) and the limit-cycle dynamics [Eq. (4)] as follows:

$$d|\psi\rangle = \left[\sum_{k=1}^K -\frac{1}{2}(L_k^2 - \langle L_k^2 \rangle) + \langle L_k \rangle (L_k - \langle L_k \rangle) \right] |\psi\rangle dt + (L_k - \langle L_k \rangle) |\psi\rangle \circ dW_k \quad (20)$$

Because Eq (20) also satisfies the norm preservation $d\|\psi\| = 0$, it can be converted into the phase equation by following the procedure of Eqs. (9)-(12), explained in Subsec. II B. Figure 3 illustrates the phase response curves corresponding to the deterministic and stochastic terms of Eq. (20) for each jump operator. It is evident from these phase response curves that the measurement backaction induces the phase bias in homodyne detection, consistent with the fact revealed in Ref. [26]. Nevertheless, since the definition of the phase does not rely on any quadratures, the phase response curves show waveform without distortion, even in homodyne detection, unlike that of the prior approach as shown in Fig. 3(b). Hence, the proposed method can represent the homodyne measurement backaction and the phase bias induced by it, while the phase is defined regardless of this bias. Applying the $U(1)$ transformation: $L_k \rightarrow \exp(i\lambda_k)L_k$ to Eq. (20), cases measuring any other quadratures can also be considered in the same way. Thus, by employing the definitions introduced in Subsec. II B, the proposed method applies to arbitrary cases of homodyne detection, including the cases where the angle, at which the quadratures are measured, is controlled via feedback, or where multiple quantum oscillators are continuously measured with different quadratures.

III. EXAMPLES

Owing to the unbiased nature of the phase in our proposed method, phase synchronization dynamics between

quantum oscillators can be analyzed without considering measurement-induced phase clusters. To demonstrate the effectiveness of our proposed method, we conduct numerical simulations wherein synchronization occurs between two uncoupled quantum oscillators subjected to common Hamiltonian noise. Noise-induced synchronization refers to the synchronization of quantum oscillators subjected to common noise, even without coupling between them. This phenomenon has been observed for various physical systems, such as uncoupled neurons [44] and single mode CO₂ lasers [45]. Theoretically, noise-induced synchronization has been analyzed in various nonlinear oscillator models by applying the phase reduction method [40] and Lyapunov exponent [46]. Furthermore, under suitable conditions, perfect synchronization between the oscillators can also be caused by common noise [40]. Recently, Schmolke and Lutz reported that a spin chain subjected to Hermitian noise synchronize [47]. In this study, we numerically simulate the case of uncoupled quantum limit-cycle oscillators subjected to common noise synchronize under continuous measurement.

Let us consider the case in which two quantum van der Pol oscillators are subjected to a Hermitian noise H_N

$$\begin{aligned} \frac{d\rho_1}{dt} &= -i[\Delta a_1^\dagger a_1 + H_N, \rho] + \gamma_g \mathcal{D}[a_1^\dagger] \rho + \gamma_d \mathcal{D}[a_1^2] \rho, \\ \frac{d\rho_2}{dt} &= -i[\Delta a_2^\dagger a_2 + H_N, \rho] + \gamma_g \mathcal{D}[a_2^\dagger] \rho + \gamma_d \mathcal{D}[a_2^2] \rho, \\ H_N &\equiv S_N \circ \xi_N(t), \end{aligned} \quad (21)$$

where S_N is an Hermitian operator; in this simulation, we specify the cases $S_N = i(a - a^\dagger)$ and $S_N = i(a^2 - a^{\dagger 2})$. In physical context, the Hermitian noise is caused by an ac-Stark shift [48] or a thermal bath [49]. To focus on the noise-induced synchronization without the phase bias caused by the measurement backaction, we use heterodyne detection for the quantum phase reduction. The Hamiltonian noise H_N can be decomposed into Lie algebra generators as $H_N = \sum_{l=1}^{N^2-1} g_{N,l} E_l$. According to Eq. (19), the phase equations corresponding to Eq. (21) can be derived as follows:

$$\begin{aligned} \frac{d\theta_1}{dt} &= \omega + v \circ \xi_1 + Z_{H_N}(\theta_1) \circ \xi_N, \\ \frac{d\theta_2}{dt} &= \omega + v \circ \xi_2 + Z_{H_N}(\theta_2) \circ \xi_N, \end{aligned} \quad (22)$$

where $Z_{H_N}(\theta) \equiv \sum_{l=1}^{N^2-1} g_l Z_l(\theta)$ is the phase response curve with respect to the Hamiltonian noise H_N .

To theoretically analyze synchronization dynamics between the two oscillators, we consider the slow limit, where the phase difference between them varies much more slowly than their frequency ω . Then, we highlight the relative phase $\phi_i \equiv \theta_i - \omega t$, which represents a disturbance from its natural frequency ω . Equation (22) is

described with respect to the relative phase ϕ as follows:

$$\begin{aligned}\frac{d\phi_1}{dt} &= v \circ \xi_1 + Z_{H_N}(\phi_1 + \omega t) \circ \xi_N, \\ \frac{d\phi_2}{dt} &= v \circ \xi_2 + Z_{H_N}(\phi_2 + \omega t) \circ \xi_N,\end{aligned}\quad (23)$$

The joint probability distribution $P(\phi_1, \phi_2, t)$ is governed by the Fokker-Planck equation [50] as follows:

$$\frac{\partial P}{\partial t} = \sum_{i=1}^2 \frac{dZ_{H_N}(\phi_i + \omega t)}{d\phi_i} Z_{H_N}(\phi_i + \omega t) + \sum_{i,j} \frac{\partial^2}{\partial \phi_i \partial \phi_j} D_{ij}, \quad (24)$$

$$D_{ij} \equiv \frac{1}{2} p^2 \delta_{ij} + \frac{1}{2} Z_{H_N}(\phi_i + \omega t) Z_{H_N}(\phi_j + \omega t), \quad (25)$$

In the slow limit, we can average the drift and diffusion coefficients in Eqs. (24) and (25) over the period T while keeping the phase difference $\phi_- \equiv \phi_1 - \phi_2$ constant (in the following, we adopt the procedure in Ref. [1, 40]).

$$\begin{aligned}\tilde{D}_{ij}(\phi_i - \phi_j) &\equiv \frac{1}{T} \int_0^{t+T} D_{ij} dt, \\ &= h(\phi_i - \phi_j) + v^2 \delta_{ij},\end{aligned}\quad (26)$$

where the correlation function $h(\phi_-)$ is defined as follows:

$$h(\phi_-) \equiv \frac{1}{2\pi} \int_0^{2\pi} Z_{H_N}(\phi_- + \phi') Z_{H_N}(\phi') d\phi'. \quad (27)$$

The correlation function $h(\phi_-)$ has maximum value at $\theta = 0$ as long as $Z_{H_N}(\theta)$ is smooth. By averaging the Fokker-Planck equation over the period T , the drift terms vanish. As shown in Eq. (26), the diffusion coefficient depends only on the phase difference ϕ_- . Then, substituting Eqs. (26) and (27) to Eq.(24), we obtain the Fokker-Planck equation averaged over period T as follows:

$$\begin{aligned}\frac{\partial}{\partial t} P(\phi_1, \phi_2, t) &= \frac{1}{2} [h(0) + v^2] \left\{ \left(\frac{\partial}{\partial \phi_1} \right)^2 + \left(\frac{\partial}{\partial \phi_2} \right)^2 \right\} P \\ &+ \frac{\partial^2}{\partial \phi_1 \partial \phi_2} [h(\phi_-) P].\end{aligned}\quad (28)$$

Moreover, to see the phase dynamics in detail, we transform the phase variables ϕ_1 and ϕ_2 to $\phi_+ \equiv \phi_1 + \phi_2$ and ϕ_- . The probability distribution $Q(\phi_-)$ is defined as $Q(\phi_-, t) \equiv \int_0^{2\pi} P(\phi_1, \phi_2, t) d\phi_+$ and the corresponding Fokker-Planck equations are represented as follows:

$$\frac{\partial Q(\phi_-)}{\partial t} = \frac{\partial^2}{\partial \phi_-^2} \{ [h(0) - h(\phi_-)] + v^2 \} Q(\phi_-, t). \quad (29)$$

Clearly, Eq. (29) has a steady state solution when $Q(\phi_-)$ is represented as

$$Q(\phi_-) = \frac{q_0}{[h(0) - h(\phi_-)] + v^2}, \quad (30)$$

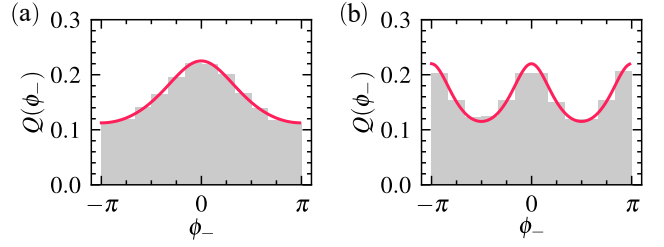


FIG. 4. Phase-difference distribution of quantum van der Pol oscillators subjected to common noise in steady state. (a) and (b) phase-difference distribution $Q(\phi_-)$ in the steady state in heterodyne detection subjected to the common noise. The gray histograms are computed from simulations of the stochastic Schrödinger equation and the red lines are computed from simulations of the phase equation. The parameters are $(\Delta, \gamma_g, \gamma_d) = (1.0, 0.2, 1.0)$. The common Hermitian noise S_N is $S_N = i(a - a^\dagger)$ for (a), $S_N = i(a^2 - a^{\dagger 2})$ for (b).

where q_0 is a normalization constant.

Although expression of the phase-difference distribution $Q(\phi_-)$ in steady state [Eq. (30)] itself is the same as that of the classical noise-induced synchronization [40], we can identify a distinction between the classical and quantum cases: the number of possible phase clusters between the two quantum oscillators is limited by their bosonic levels. In classical cases, considering common noise with higher-order terms allowed for an arbitrarily large number of phase clusters between two oscillators. As shown in Eq. (30), the phase distribution in the steady state depends on the correlation function $h(\phi_-)$. For the quantum van der Pol oscillators in heterodyne detection, the phase response curves are given as trigonometric functions with the modes of $N - 1$ or less. For instance, when $S_N = i(a - a^\dagger)$ or $i(a^2 - a^{\dagger 2})$, the corresponding phase response curve is a first or second harmonic, resulting in a synchronized state or cluster state in steady state as shown in Figs. 4(a) and (b). The correlation function $h(\phi_-)$ can be represented by a linear combination of the trigonometric functions with modes of $N - 1$ or less. Hence the number of possible phase clusters in response to an external perturbation is restricted by their bosonic levels, unlike the classical case.

IV. CONCLUSION

In this study, we extend Lie algebraic quantum phase reduction [26] to heterodyne detection, where all quadrature observables are uniformly measured. Averaging out the measurement backaction, the proposed method derives an unbiased phase equation in the absence of measurement-induced phase clusters. Moreover, our proposed method also applies to arbitrary cases of homodyne detection, including the scenario where the quadratures are modified during the time evolution. Using the proposed method, we conduct numerical simulations where uncoupled quantum van der Pol oscillators subjected to

common noise exhibit synchronization. Recently, various phenomena intrinsic to quantum oscillators have been reported in field of quantum synchronization, spurring the demand for their analysis [51–53]. In studies of classical synchronization, the extensions of phase reduction theory have been developed to increase its effectiveness for complex synchronization dynamics [54, 55]. Incorporating these techniques to Lie algebraic quantum phase reduction may enhance its adaptability to the synchronization phenomena specific to quantum oscillators.

Appendix A: Norm preservation of limit-cycle equation

To ensure the limit-cycle solution of the stochastic Schrödinger equation to be a pure-state trajectory, its deterministic term must satisfy the norm preservation condition $\|\psi\rangle\| = 1$. However, it should be noted that the deterministic terms of the stochastic differential equations varies with the choice of stochastic calculus for their evaluation. We establish that the Stratonovich calculus uniquely satisfies the norm preservation of the limit-cycle dynamics. Considering an arbitrary stochastic calculus, we evaluate the stochastic Schrödinger equation at an arbitrary time $t + pdt$ during $[t, t + dt]$, where $0 \leq p \leq 1$ ($p = 0$ in the Ito calculus and $p = 1/2$ in the Stratonovich calculus). When the stochastic Schrödinger equation is evaluated at time $t + pdt$, it is represented as follows:

$$\begin{aligned} d|\psi(t)\rangle &= \left[-iH_{\text{eff}} + \sum_{k=1}^K \langle L_k^\dagger \rangle L_k - \frac{1}{2} \langle L_k^\dagger \rangle \langle L_k \rangle \right] |\psi(t + pdt)\rangle dt \\ &+ p \left[\langle L_k^\dagger L_k \rangle - \langle L_k^\dagger \rangle \langle L_k \rangle \right] |\psi(t + pdt)\rangle dt \\ &+ (L_k - \langle L_k \rangle) |\psi(t + pdt)\rangle dZ^*(t), \end{aligned} \quad (\text{A1})$$

where terms less than $O(dt)$ are neglected. The time derivative of the norm $\|\psi\rangle\|$ under the deterministic terms of Eq. (A1) is described as follows:

$$\begin{aligned} d(\langle\psi|\psi\rangle) &= (\langle\psi| + d\langle\psi|)(|\psi\rangle + d|\psi\rangle) - \langle\psi|\psi\rangle \\ &= (d\langle\psi|)|\psi\rangle + \langle\psi|(d|\psi\rangle) + (d\langle\psi|)(d|\psi\rangle) \\ &= (2p - 1) \sum_{k=1}^K \left[\langle L_k^\dagger L_k \rangle - \langle L_k^\dagger \rangle \langle L_k \rangle \right] dt, \end{aligned} \quad (\text{A2})$$

Clearly, the norm preservation $d\|\psi\rangle\| = 0$ for an arbitrary state $|\psi\rangle$ is satisfied only if $p = 1/2$, the Stratonovich calculus.

Appendix B: Generators of $SU(N)$

The generators of $SU(N)$ correspond to generalized Gell-Mann matrices. The generalized Gell-Mann matrices

are composed of off-diagonal matrices $f_{k,l}$ and diagonal matrices $h_{k,l}$.

$$\Lambda_{j,k} \equiv \begin{cases} \text{for } 1 \leq j < k \leq N \\ O_{k,j} + O_{j,k}, \\ \text{for } 1 \leq k < j \leq N \\ -i(O_{j,k} - O_{k,j}), \\ \text{for } 1 \leq j = k \leq N - 1 \\ \sqrt{\frac{2}{j(j+1)}} \left(\sum_{l=1}^j O_{l,l} - jO_{j+1,j+1} \right), \end{cases} \quad (\text{B1})$$

where $O_{j,k}$ is the matrix with 1 in the jk -th entry and 0 elsewhere. The generators $E_{j,k}$ are defined so that they are normalized with respect to the trace norm:

$$E_{j,k} \equiv \frac{1}{\sqrt{\text{Tr}[\Lambda_{j,k}^2]}} \Lambda_{j,k}, \quad (\text{B2})$$

Appendix C: Conversion between Ito and Stratonovich calculi

Typically, a stochastic differential equation is represented by two different forms, the Ito and Stratonovich forms, which are given as follows:

$$f(t)dW(t) \equiv f(t)(W(t+dt) - W(t)), \quad (\text{C1})$$

$$f(t) \circ dW(t) \equiv f\left(t + \frac{dt}{2}\right)(W(t+dt) - W(t)), \quad (\text{C2})$$

where $W(t)$ is a Wiener process. In the Stratonovich interpretation, a calculus is performed at the midpoint of the interval $[t, t + dt]$. Moreover, the two forms can be converted to each other using the following transformation:

$$f(t) \circ dW(t) = f(t)dW(t) + \frac{1}{2}df(t)dW(t). \quad (\text{C3})$$

The conversion of Eq. (C3) is performed according to the Ito rule:

$$dW(t)^2 = dt, \quad (\text{C4})$$

$$dW(t)dt = 0. \quad (\text{C5})$$

Appendix D: Limit-cycle solution of quantum van der Pol oscillator in heterodyne detection

To show that the limit-cycle solution of the quantum van der Pol oscillator is a harmonic oscillation in heterodyne detection, we provide a brief proof for it. We define a unitary transformation $R(\lambda)$ corresponding to harmonic oscillation as $R(\lambda) \equiv \exp(-ia^\dagger a \lambda)$. According to Eq. (4), dynamics of limit cycle for quantum van der Pol oscillators [Eq. (18)] is represented as follows:

$$\begin{aligned} d|\psi\rangle &= \left[-ia^\dagger a - \frac{1}{2}(\gamma_g a a^\dagger + \gamma_a a^{\dagger 2} a^2) + \gamma_g \langle a \rangle (a^\dagger - \langle a^\dagger \rangle) \right. \\ &\quad \left. + \gamma_a \langle a^{\dagger 2} \rangle (a^2 - \langle a^2 \rangle) \right] |\psi\rangle dt. \end{aligned} \quad (\text{D1})$$

By performing this unitary transformation on the quantum state $|\psi\rangle$ in Eq. (D1) of quantum van der Pol oscillators, we find $R(|\psi\rangle + d|\psi\rangle) = R(\lambda)|\psi\rangle + d(R(\lambda)|\psi\rangle)$, that is, time evolution in Eq. (D1) and the unitary transformation $R(\lambda)$ commute. By introducing the operator $C(\beta)$ as $C(\beta)|\psi(t)\rangle = |\psi(t+\beta)\rangle$ under Eq. (D1), it is clear $C(\beta)R(\lambda)|\psi\rangle = R(\lambda)C(\beta)|\psi\rangle$. Using this relation in the limit-cycle solution $|\psi_0(\theta)\rangle$, we can derive

$$\begin{aligned} C(\beta)R(\lambda)|\psi_0(\theta)\rangle &= R(\lambda)C(\beta)|\psi_0(\theta)\rangle \\ &= R(\lambda)|\psi_0(\theta + \omega\beta)\rangle. \end{aligned} \quad (\text{D2})$$

To take $\beta \rightarrow \infty$, the left-hand side of Eq. (D2) converges on the limit-cycle solution $|\psi_0\rangle$. Thus, the limit-cycle solution $|\psi_0\rangle$ is a harmonic oscillation and is described as an circle on xp plane.

Appendix E: Phase response curve of quantum van der Pol oscillator in heterodyne detection

We prove that in heterodyne detection, the phase response curves corresponding to jump operators in the quantum van der Pol oscillators are constant white noise. Unitary transformation $R(\lambda) = \exp(i\lambda a^\dagger a)$ and annihilation and creation operators satisfy $R(\lambda)a = e^{i\lambda}aR(\lambda)$.

Using this fact, when we define the derivative of quantum states with respect to perturbations as $d|\psi\rangle = (a^\dagger - \langle a^\dagger \rangle)|\psi\rangle dt$, we can derive

$$\begin{aligned} d[R(\lambda)|\psi\rangle] &= e^{-i\lambda}d|\psi\rangle \\ &= (a^\dagger e^{-i\lambda} - \langle a^\dagger e^{-i\lambda} \rangle)|\psi\rangle dt. \end{aligned} \quad (\text{E1})$$

According to Appendix D, unitary transformation $R(\lambda)$ and dynamics of limit cycle defined by Eq. (4) commute. Employing this and Eq. (E1), we derive $Z_r(\lambda) = \cos(\lambda)Z_r(0) - \sin(\lambda)Z_i(0)$ where $Z_r(\theta)$ and $Z_i(\theta)$ are phase response curves with respect to perturbations of a^\dagger and ia^\dagger , respectively. Then, we find that $Z_r(\theta)$ can be represented as $Z_r(\theta) = c \cos(\theta + \theta_0)$ where θ_0 is constant. Considering the case where $\lambda = \pi/2$ in Eq. (E1), it can be easily deduced that $Z_r(\lambda) = -Z_i(\lambda - \pi/2)$. Finally, we can obtain $\sqrt{[Z_r(\theta)dW_1]^2 + [Z_i(\theta)dW_2]^2} = \sqrt{2}cdW$. A similar discussion can be applied to a jump operator a^2 .

ACKNOWLEDGMENTS

This work was supported by JSPS KAKENHI Grant No. JP22H03659.

-
- [1] Y. Kuramoto, *Chemical Oscillations, Waves, and Turbulence* (Springer, New York, 1984).
 - [2] A. Winfree, *The Geometry of Biological Time*, 2nd ed. (Springer, New York, 2001).
 - [3] E. Izhikevich, *Dynamical Systems in Neuroscience* (MIT Press, Cambridge, Massachusetts, 2007).
 - [4] S. H. Strogatz, *Nonlinear Dynamics and Chaos: with Applications to Physics, Biology, Chemistry, and Engineering* (CRC press, Boca Raton, 2018).
 - [5] A. M. Hriscu and Y. V. Nazarov, Quantum synchronization of conjugated variables in a superconducting device leads to the fundamental resistance quantization, *Phys. Rev. Lett.* **110**, 097002 (2013).
 - [6] S. E. Nigg, Observing quantum synchronization blockade in circuit quantum electrodynamics, *Phys. Rev. A* **97**, 013811 (2018).
 - [7] N. Lörch, J. Qian, A. Clerk, F. Marquardt, and K. Hammerer, Laser theory for optomechanics: limit cycles in the quantum regime, *Phys. Rev. X* **4**, 011015 (2014).
 - [8] T. Weiss, A. Kronwald, and F. Marquardt, Noise-induced transitions in optomechanical synchronization, *New J. Phys.* **18**, 013043 (2016).
 - [9] J. Javaloyes, M. Perrin, and A. Politi, Collective atomic recoil laser as a synchronization transition, *Phys. Rev. E* **78**, 011108 (2008).
 - [10] M. Xu and M. J. Holland, Conditional Ramsey spectroscopy with synchronized atoms, *Phys. Rev. Lett.* **114**, 103601 (2015).
 - [11] T. Feldmann and R. Kosloff, Characteristics of the limit cycle of a reciprocating quantum heat engine, *Phys. Rev. E* **70**, 046110 (2004).
 - [12] Y. Rezek and R. Kosloff, Irreversible performance of a quantum harmonic heat engine, *New J. Phys.* **8**, 83 (2006).
 - [13] A. U. C. Hardal, N. Aslan, C. M. Wilson, and O. E. Müstecaplıoğlu, Quantum heat engine with coupled superconducting resonators, *Phys. Rev. E* **96**, 062120 (2017).
 - [14] N. Jaseem, M. Hajdušek, V. Vedral, R. Fazio, L.-C. Kwek, and S. Vinjanampathy, Quantum synchronization in nanoscale heat engines, *Phys. Rev. E* **101**, 020201 (2020).
 - [15] N. Crescini, S. Cailleaux, W. Guichard, C. Naud, O. Buisson, K. W. Murch, and N. Roch, Evidence of dual Shapiro steps in a Josephson junction array, *Nat. Phys.* **1** (2023).
 - [16] M. E. Ladd, P. Bachert, M. Meyerspeer, E. Moser, A. M. Nagel, D. G. Norris, S. Schmitter, O. Speck, S. Straub, and M. Zaiss, Pros and cons of ultra-high-field MRI/MRS for human application, *Prog. Nucl. Magn. Reson. Spectrosc.* **109**, 1 (2018).
 - [17] Y. Liu, R. Quan, X. Xiang, H. Hong, M. Cao, T. Liu, R. Dong, and S. Zhang, Quantum clock synchronization over 20-km multiple segmented fibers with frequency-correlated photon pairs and hom interference, *Appl. Phys. Lett.* **119**, 144003 (2021).
 - [18] E. Schwarzthans, M. P. E. Lock, P. Erker, N. Friis, and M. Huber, Autonomous temporal probability concentration: Clockworks and the second law of thermodynamics, *Phys. Rev. X* **11**, 011046 (2021).
 - [19] A. Roulet and C. Bruder, Synchronizing the smallest possible system, *Phys. Rev. Lett.* **121**, 053601 (2018).

- [20] A. Parra-López and J. Bergli, Synchronization in two-level quantum systems, *Phys. Rev. A* **101**, 062104 (2020).
- [21] T. E. Lee and H. R. Sadeghpour, Quantum synchronization of quantum van der Pol oscillators with trapped ions, *Phys. Rev. Lett.* **111**, 234101 (2013).
- [22] S. Walter, A. Nunnenkamp, and C. Bruder, Quantum synchronization of a driven self-sustained oscillator, *Phys. Rev. Lett.* **112**, 094102 (2014).
- [23] A. W. Laskar, P. Adhikary, S. Mondal, P. Katiyar, S. Vinjanampathy, and S. Ghosh, Observation of quantum phase synchronization in spin-1 atoms, *Phys. Rev. Lett.* **125**, 013601 (2020).
- [24] P. Kongkhambut, J. Skulte, L. Mathey, J. G. Cosme, A. Hemmerich, and H. Kefler, Observation of a continuous time crystal, *Science* **377**, 670 (2022).
- [25] M. Koppenhöfer, C. Bruder, and A. Roulet, Quantum synchronization on the IBM Q system, *Phys. Rev. Res.* **2**, 023026 (2020).
- [26] W. Setoyama and Y. Hasegawa, Lie algebraic quantum phase reduction, *Phys. Rev. Lett.* **132**, 093602 (2024).
- [27] N. Gisin and I. C. Percival, The quantum-state diffusion model applied to open systems, *J. Phys. A: Math. Gen.* **25**, 5677 (1992).
- [28] C. Gardiner, P. Zoller, and P. Zoller, *Quantum Noise: A Handbook of Markovian and Non-Markovian Quantum Stochastic Methods with Applications to Quantum Optics* (Springer Science & Business Media, 2004).
- [29] A. Barchielli and M. Gregoratti, *Quantum Trajectories and Measurements in Continuous Time: the Diffusive Case*, Vol. 782 (Springer, Berlin, 2009).
- [30] Y. Kato, N. Yamamoto, and H. Nakao, Semiclassical phase reduction theory for quantum synchronization, *Phys. Rev. Res.* **1**, 033012 (2019).
- [31] G. Lindblad, On the generators of quantum dynamical semigroups, *Commun. Math. Phys.* **48**, 119 (1976).
- [32] H. Breuer, F. Petruccione, and S. Petruccione, *The Theory of Open Quantum Systems* (Oxford University Press, New York, 2002).
- [33] H. Carmichael, *An Open Systems Approach to Quantum Optics: Lectures Presented at the Université Libre de Bruxelles*, Lecture Notes in Physics Monographs (Springer, Berlin; New York, 2009).
- [34] H. M. Wiseman and G. J. Milburn, *Quantum measurement and control* (Cambridge university press, 2009).
- [35] K. Jacobs and D. A. Steck, A straightforward introduction to continuous quantum measurement, *Contemp. Phys.* **47**, 279 (2006).
- [36] C. Guerlin, J. Bernu, S. Deleglise, C. Sayrin, S. Gleyzes, S. Kuhr, M. Brune, J.-M. Raimond, and S. Haroche, Progressive field-state collapse and quantum non-demolition photon counting, *Nature* **448**, 889 (2007).
- [37] K. Murch, S. Weber, C. Macklin, and I. Siddiqi, Observing single quantum trajectories of a superconducting quantum bit, *Nature* **502**, 211 (2013).
- [38] M. Rossi, D. Mason, J. Chen, and A. Schliesser, Observing and verifying the quantum trajectory of a mechanical resonator, *Phys. Rev. Lett.* **123**, 163601 (2019).
- [39] J. N. Teramae, H. Nakao, and G. B. Ermentrout, Stochastic phase reduction for a general class of noisy limit cycle oscillators, *Phys. Rev. Lett.* **102**, 194102 (2009).
- [40] H. Nakao, K. Arai, and Y. Kawamura, Noise-induced synchronization and clustering in ensembles of uncoupled limit-cycle oscillators, *Phys. Rev. Lett.* **98**, 184101 (2007).
- [41] K. Yoshimura and K. Arai, Phase reduction of stochastic limit cycle oscillators, *Phys. Rev. Lett.* **101**, 154101 (2008).
- [42] D. Goldobin and A. Pikovsky, Synchronization of self-sustained oscillators by common white noise, *Physica A* **351**, 126 (2005).
- [43] H. Nakao, Phase reduction approach to synchronisation of nonlinear oscillators, *Contemporary Physics* **57**, 188 (2016).
- [44] A. B. Neiman and D. F. Russell, Synchronization of noise-induced bursts in noncoupled sensory neurons, *Phys. Rev. Lett.* **88**, 138103 (2002).
- [45] C. S. Zhou, J. Kurths, E. Allaria, S. Boccaletti, R. Meucci, and F. T. Arecchi, Constructive effects of noise in homoclinic chaotic systems, *Phys. Rev. E* **67**, 066220 (2003).
- [46] C. Zhou and J. Kurths, Noise-induced synchronization and coherence resonance of a Hodgkin–Huxley model of thermally sensitive neurons, *Chaos* **13**, 401 (2003).
- [47] F. Schmolke and E. Lutz, Noise-induced quantum synchronization, *Phys. Rev. Lett.* **129**, 250601 (2022).
- [48] C. Maier, T. Brydges, P. Jurcevic, N. Trautmann, C. Hempel, B. P. Lanyon, P. Hauke, R. Blatt, and C. F. Roos, Environment-assisted quantum transport in a 10-qubit network, *Phys. Rev. Lett.* **122**, 050501 (2019).
- [49] B. Karimi and J. P. Pekola, Correlated versus uncorrelated noise acting on a quantum refrigerator, *Phys. Rev. B* **96**, 115408 (2017).
- [50] H. Risken, Fokker-Planck equation, in *The Fokker-Planck Equation* (Springer, 1996) pp. 63–95.
- [51] N. Lörch, E. Amitai, A. Nunnenkamp, and C. Bruder, Genuine quantum signatures in synchronization of anharmonic self-oscillators, *Phys. Rev. Lett.* **117**, 073601 (2016).
- [52] N. Lörch, S. E. Nigg, A. Nunnenkamp, R. P. Tiwari, and C. Bruder, Quantum synchronization blockade: Energy quantization hinders synchronization of identical oscillators, *Phys. Rev. Lett.* **118**, 243602 (2017).
- [53] P. Solanki, F. M. Mehdi, M. Hajdušek, and S. Vinjanampathy, Symmetries and synchronization blockade, *Phys. Rev. A* **108**, 022216 (2023).
- [54] W. Kurebayashi, S. Shirasaka, and H. Nakao, Phase reduction method for strongly perturbed limit cycle oscillators, *Phys. Rev. Lett.* **111**, 214101 (2013).
- [55] D. Wilson, Phase-amplitude reduction far beyond the weakly perturbed paradigm, *Phys. Rev. E* **101**, 022220 (2020).